

TABLE II: Rate Constants for the Reactions of Sulfur Radicals with NO₂ at Room Temperature

reaction	rate const, cm ³ molecule ⁻¹ s ⁻¹	ref
S + NO ₂ → SO + NO	6.5 × 10 ⁻¹¹	46
HS + NO ₂ → HSO + NO	6.7 × 10 ⁻¹¹	38
CH ₃ S + NO ₂ → CH ₃ SO + NO	5.1 × 10 ⁻¹¹	this work
CH ₃ SS + NO ₂ → products	1.8 × 10 ⁻¹¹	this work
SO + NO ₂ → SO ₂ + NO	1.4 × 10 ⁻¹¹	46
HSO + NO ₂ → products	9.6 × 10 ⁻¹²	43
CH ₃ SO + NO ₂ → products	1.2 × 10 ⁻¹¹	this work
CH ₃ SSO + NO ₂ → products	4.5 × 10 ⁻¹²	this work

would give NO by reaction with NO₂.

The two rate constants k_1 and k_2 measured here support the trend reported by Lovejoy et al.⁴³ They noted that the rate constants of the R-S + NO₂ reactions are about 6 × 10⁻¹¹ cm³ molecule⁻¹ s⁻¹ and that those of the RSO + NO₂ reactions are about 1.2 × 10⁻¹¹ cm³ molecule⁻¹ s⁻¹. Some relevant rate constant values are summarized in Table II. As one may have expected, the rate constants of the reaction of CH₃SS (k_3) and CH₃SSO (k_4) with NO₂ do not follow the rule, but it appears that the ratio k_3/k_4 follows the pattern observed for the other RS/RSO.

(45) Clyne, M. A. A.; Whitefield, P. D. *J. Chem. Soc., Faraday Trans. 2* 1979, 75, 1327.

The atmospheric loss rates of CH₃S by oxidation by O₂, NO₂, and O₃ have already been discussed by Tyndall and Ravishankara.^{26,46} They suggested that the reaction of CH₃S with O₃ yielded CH₃SO and that the subsequent reaction of CH₃SO with O₃ regenerated CH₃S in one or several steps and that therefore the reaction with O₃ would not result in a loss of CH₃S. Only an upper limit of 2.5 × 10⁻¹⁸ cm³ molecule⁻¹ s⁻¹ is available for the rate constant of the CH₃S + O₂ reaction,²⁶ and this reaction could still be the main gas-phase loss of CH₃S in the atmosphere.

The present determination of k_2 allows the calculation of the atmospheric first-order rate constant of the reaction of CH₃SO with NO₂. In remote areas ([NO₂] ≈ 3 × 10⁸ molecules cm⁻³), the rate constant is about 4 × 10⁻³ s⁻¹, and in moderately polluted areas ([NO₂] ≈ 3 × 10¹⁰ cm⁻³), the rate constant is about 0.4 s⁻¹. Further studies of the reactions of CH₃SO with O₂ and O₃ are necessary to evaluate the atmospheric fate of CH₃SO.

Acknowledgment. This work was supported by NOAA as part of the National Acid Precipitation Assessment Program. Numerous stimulating and helpful discussions were held with E. R. Lovejoy over the course of this study.

(46) DeMore, W. B.; Molina, M. J.; Sander, S. P.; Golden, D. M.; Hampson, R. F.; Kurylo, M. J.; Howard, C. J.; Ravishankara, A. R. *Chemical Kinetics and Photochemical Data for Use in Stratospheric Modeling, Evaluation No. 8*; Jet Propulsion Laboratory Publication 87-41, 1987.

(47) Tyndall, G. S.; Ravishankara, A. R. *J. Phys. Chem.* 1989, 93, 4707.

Kinetics of Sequential Energy-Transfer Processes

M. N. Berberan-Santos* and J. M. G. Martinho

Centro de Química-Física Molecular, Instituto Superior Técnico, 1096 Lisboa Codex, Portugal
(Received: November 21, 1989)

The kinetics of sequential excitation energy transfer in a four-species system have been studied and numerically exemplified for the case of a $t^{-1/2}$ dependence of the rate coefficients. It has been shown that previous treatments based on differential equations are incorrect owing to improper use of the rate coefficient derived for δ -pulse excitation.

Introduction

Sequential electronic energy transfer is an important process of frequency conversion and occurs in photosynthetic systems as a means to increase light collection performance. For instance, the wavelength-resolved fluorescence emission of the accessory pigments and chlorophyll *a* in the alga *Porphyridium cruentum* shows¹ that successive processes of energy transfer occur between the pigments until the electronic excitation energy reaches a reaction center, the pathway for 530-nm excitation being phycoerythrin to phycocyanin to allophycocyanin to chlorophyll *a* to reaction center. Recently, sequential energy transfer was also studied in Langmuir-Blodgett multilayers.²

The first kinetic model for the process of sequential transfer was that of Porter et al.¹ and consisted of a kinetic scheme of consecutive, irreversible transfers with rate coefficients having a $t^{-1/2}$ time dependence. These results were reproduced for other algae^{3,4} and also used for Langmuir-Blodgett multilayers.² A

major assumption leading to the $t^{-1/2}$ time dependence⁵ is nevertheless not verified in these systems, namely the random distribution of acceptors in three dimensions.⁶

In this work, we present a more general treatment of the kinetics of irreversible sequential transfer (very weak coupling limit), numerically exemplified for the case of a $t^{-1/2}$ dependence of the rate coefficients.

The Kinetic Model

A general decay law for each of the species participating in the energy-transfer sequence can be written, for delta production, as

$$f_i(t) = \exp\left(-\frac{t}{\tau_i}\right) \exp\left(-\int_0^t k_{ib}(u) du\right) \quad (1)$$

where τ_i is the intrinsic lifetime and $k_{ib}(t)$ the rate coefficient for energy transfer in step *i*. In the special case of a three-dimensional rigid solution of randomly distributed acceptors, it takes the form

(1) Porter, G.; Tredwell, C. J.; Searle, G. F. W.; Barber, J. *Biochim. Biophys. Acta* 1978, 501, 232-245.

(2) Yamazaki, I.; Tamai, N.; Yamazaki, T.; Murakami, A.; Mimuro, M.; Fujita, Y. *J. Phys. Chem.* 1988, 92, 5035-5044.

(3) Holzwarth, A. R.; Wendler, J.; Wehrmeyer, W. *Photochem. Photobiol.* 1982, 36, 479-487.

(4) Yamazaki, I.; Mimuro, M.; Murao, T.; Yamazaki, T.; Yoshihara, K.; Fujita, Y. *Photochem. Photobiol.* 1984, 39, 233-240.

(5) (a) Förster, T. *Z. Naturforsch.* 1949, 4a, 321. (b) Blumen, A.; Manz, J. *J. Chem. Phys.* 1979, 71, 4694.

(6) Hanzlik, C. A.; Hancock, L. E.; Knox, R. S.; Guard-Friar, D.; Maccoll, R. *J. Lumin.* 1985, 34, 99-106.

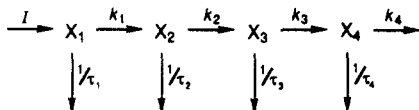
$$k_{ib}(t) = A_i/t^{1/2} \quad (2)$$

with⁵

$$A_i = \frac{2\pi^{3/2}R_{0i}^3N_A C_{i+1}}{3\tau_i^{1/2}} \quad (3)$$

where R_{0i} is the critical distance for transfer (Förster radius) from i to $i + 1$, N_A Avogadro's number, and C_{i+1} the acceptor concentration.

Consider the following kinetic scheme, where $k_i(t)$ ($i = 1, \dots, 4$) are appropriate rate coefficients and X_i ($i = 1, \dots, 4$) the populations of the different species, and $I(t)$ is the rate of production of excited species X_1 .



The time evolution of the excited-state populations is given by the following set of rate equations

$$\frac{dX_1}{dt} = I(t) - \left(\frac{1}{\tau_1} + k_1(t) \right) X_1 \quad (4)$$

$$\frac{dX_2}{dt} = k_1(t)X_1 - \left(\frac{1}{\tau_2} + k_2(t) \right) X_2 \quad (5)$$

$$\frac{dX_3}{dt} = k_2(t)X_2 - \left(\frac{1}{\tau_3} + k_3(t) \right) X_3 \quad (6)$$

$$\frac{dX_4}{dt} = k_3(t)X_3 - \left(\frac{1}{\tau_4} + k_4(t) \right) X_4 \quad (7)$$

Now it should be noted that rate coefficients $k_i(t)$ in eqs 4–7 are not generally equal to rate coefficients k_{ib} of eq 1. In fact these are related by (see Appendix)

$$k_i(t) = \frac{P_i \otimes (k_{ib}f_i)}{P_i \otimes f_i} \quad (8)$$

where P_i is the production rate of X_i . Consideration of the rate eqs 4–7 leads to ($i > 1$)

$$k_i(t) = \frac{k_{i-1}X_{i-1} \otimes k_{ib}f_i}{k_{i-1}X_{i-1} \otimes f_i} = \frac{k_{i-1}X_{i-1} \otimes k_{ib}f_i}{X_i} \quad (9)$$

which are different from the corresponding k_{ib} . For the calculation of the X_i , integration of the differential equations is not really necessary, as it is known that X_i is simply given by the convolution of $k_{i-1}X_{i-1}$ with f_i and therefore a recurrence procedure based on eq 9 is possible

$$X_1 = I \otimes f_1 \quad (10)$$

$$X_2 = k_1X_1 \otimes f_2 = I \otimes k_{1b}f_1 \otimes f_2 \quad (11)$$

$$X_3 = k_2X_2 \otimes f_3 = I \otimes k_{1b}f_1 \otimes k_{2b}f_2 \otimes f_3 \quad (12)$$

$$X_4 = k_3X_3 \otimes f_4 = I \otimes k_{1b}f_1 \otimes k_{2b}f_2 \otimes k_{3b}f_3 \otimes f_4 \quad (13)$$

Notwithstanding, the obtained X_i are the solutions of the differential eqs 4–7. In previous studies of sequential energy-transfer processes the rate coefficients k_i and k_{ib} were erroneously assumed to be equal.^{1–4} In order to exemplify the differences between the differential (rate coefficients equal to k_{ib}) and convolution (rate coefficients given by eq 8) treatments, numerical calculations were performed using the experimental data obtained by Porter et al.¹ However, it is not implied that the assumed form for $k(t)$, namely eq 2, is a good approximation for photosynthetic systems.⁶

Numerical Results

The solution of the differential eqs 4–7 for δ -pulse production of X_1 , considering infinite lifetimes (reasonable assumption for

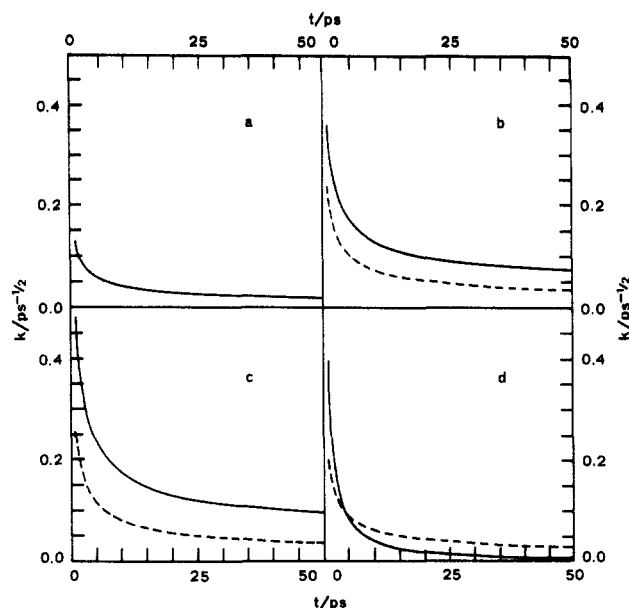


Figure 1. Comparison of the time-dependent rate coefficients, k_1 (a), k_2 (b), k_3 (c), k_4 (d) obtained from convolution (—) and for δ -pulse excitation (---). The numerical coefficients are those of ref 1. $A_1 = 0.13$ ps^{-1/2}, $A_2 = 0.24$ ps^{-1/2}, $A_3 = 0.26$ ps^{-1/2}, $A_4 = 0.20$ ps^{-1/2}.

fast energy-transfer processes) and when $A_i/t^{1/2}$ is substituted for $k_i(t)$, is^{1–4}

$$X_1 = \exp(-2A_1t^{1/2}) \quad (14)$$

$$X_2 = \frac{A_1}{A_2 - A_1} [\exp(-2A_1t^{1/2}) - \exp(-2A_2t^{1/2})] \quad (15)$$

$$X_3 = \frac{A_1A_2}{A_2 - A_1} \left[\frac{\exp(-2A_1t^{1/2}) - \exp(-2A_3t^{1/2})}{A_3 - A_1} - \frac{\exp(-2A_2t^{1/2}) - \exp(-2A_3t^{1/2})}{A_3 - A_2} \right] \quad (16)$$

$$X_4 = \frac{A_1A_2A_3}{A_2 - A_1} \left[\frac{\exp(-2A_1t^{1/2}) - \exp(-2A_4t^{1/2})}{(A_4 - A_1)(A_3 - A_1)} - \frac{\exp(-2A_4t^{1/2}) - \exp(-2A_3t^{1/2})}{(A_3 - A_4)(A_3 - A_1)} - \frac{\exp(-2A_4t^{1/2}) - \exp(-2A_2t^{1/2})}{(A_2 - A_4)(A_3 - A_2)} + \frac{\exp(-2A_4t^{1/2}) - \exp(-2A_3t^{1/2})}{(A_3 - A_4)(A_3 - A_2)} \right] \quad (17)$$

Nevertheless, this procedure is not correct as the rate coefficients used are only valid for δ -production of each donor species.

Figure 1 shows the plot of the rate coefficients $k_i(t)$ versus time given by eq 9 and compares the values with the ones calculated from $k_{ib} = A_i/t^{1/2}$, obtained from the fitting of the experimental results to eqs 14–17.¹ The $k_i(t)$ ($i > 1$) are higher than the corresponding k_{ib} for short times, decreasing with time to closer values. This reflects the importance of the production term in each step of energy transfer. The decay curves presented in Figure 2, computed from eqs 10–13 and 14–17, reflect the time dependence of the rate coefficients. The rise time of the population of X_i ($i > 1$) is faster when the appropriate values of the rate coefficients, $k(t)$, are used, reflecting the larger values of the rate coefficients for short times.

Conclusions

The usual time-dependent rate coefficients, obtained for δ -pulse excitation, are not valid for other types of excitation, as occurs

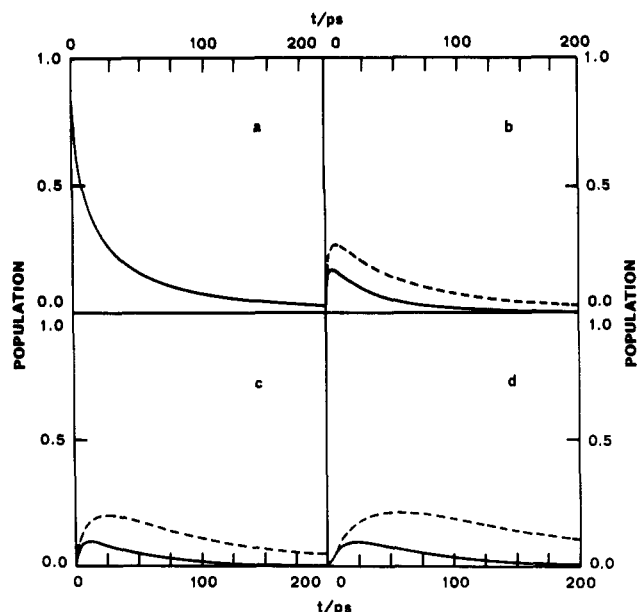


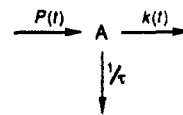
Figure 2. Comparison of the time evolution of the populations of the species X_1 (a), X_2 (b), X_3 (c), X_4 (d) as obtained from convolution (—) and from differential equations with k_δ rate coefficients (---).

in consecutive processes of transfer. This was numerically shown for the case of an inverse square root of time dependence of the rate coefficient, where significant differences were obtained. The treatment presented can be applied to other systems once the rate coefficients for δ -pulse excitation are known for the various elementary steps of the kinetic scheme.

Acknowledgment. This work was developed under project CQFM-1 of Instituto Nacional de Investigaço Cientfica. Financial support from Junta Nacional de Investigaço Cientfica e Tecnolgica is acknowledged.

Appendix

Consider the kinetic scheme



where A is some excited state species, $P(t)$ is its production rate, and $k(t)$ is some time-dependent coefficient describing the deactivation process. According to classical kinetics, the associated differential equation is

$$\frac{dA}{dt} = P - \left(\frac{1}{\tau} + k \right) A \quad (\text{A1})$$

However, the time-dependent rate coefficients usually derived are obtained for δ -pulse excitation conditions, that is,

$$\frac{dA}{dt} = \delta(t) - \left(\frac{1}{\tau} + k_\delta \right) A \quad (\text{A2})$$

The solution of eq A2 is ($t > 0$)

$$A_\delta = f = \exp\left(-\frac{t}{\tau}\right) \exp\left(-\int_0^t k_\delta(u) du\right) \quad (\text{A3})$$

We now show that $k(t)$ for a $P(t)$ generation (eq A1) generally differs from $k_\delta(t)$. If the system under consideration is linear, the response to a generation rate $P(t)$ can be considered to be a sum of δ -pulse responses; hence

$$A = P \otimes f = \int_0^t P(u) f(t-u) du \quad (\text{A4})$$

Solving eq A1 for $k(t)$ and substituting A as given by eq A4,

$$k = -\frac{P \otimes \frac{df}{dt}}{P \otimes f} - \frac{1}{\tau} \quad (\text{A5})$$

and using eq A3,

$$k = \frac{P \otimes (k_\delta f)}{P \otimes f} \quad (\text{A6})$$

This clearly differs from k_δ , unless k_δ is time independent.

Primary Donor State Mode Structure and Energy Transfer in Bacterial Reaction Centers

S. G. Johnson, D. Tang, R. Jankowiak, J. M. Hayes, G. J. Small,*

Ames Laboratory–USDOE and Department of Chemistry, Iowa State University, Ames, Iowa 50011

and D. M. Tiede

Chemistry Division, Argonne National Laboratory, Argonne, Illinois 60439 (Received: November 21, 1989; In Final Form: January 24, 1990)

Temperature-dependent photochemical hole burning data for P870 of *Rhodobacter sphaeroides* reaction centers (RC) are reported which lead to a determination for the mean frequency of the protein phonons which couple to the optical transition. Utilization of this frequency, $\omega_m \sim 25\text{--}30\text{ cm}^{-1}$, together with improved functions for the single site (RC) absorption line shape and inhomogeneous broadening is shown to lead to significant improvement in the theoretical fits to the hole and absorption spectra (including those of P960 of *Rhodospseudomonas viridis*). Time-dependent P870 hole spectra are reported which provide additional evidence that the previously observed zero-phonon hole is an intrinsic feature of P870 for active RC. Transient spectra obtained by laser excitation into the accessory Q_y -absorption bands of the RC are presented which show an absence of both line narrowing and a dependence on the location of the excitation frequency. These results, which are consistent with ultrafast energy-transfer processes from the accessory states, are discussed in terms of earlier time domain data.

I. Introduction

Recently the underlying structures of the primary donor state (special pair) absorption profiles P870 and P960 of the bacterial reaction centers (RC) from *Rhodospseudomonas viridis* and *Rhodobacter sphaeroides* were revealed by transient photochem-

ical hole burning experiments.^{1,2} Both are dominated by a fairly lengthy Franck–Condon progression in an *intermolecular* spe-

(1) Johnson, S. G.; Tang, D.; Jankowiak, R.; Hayes, J. M.; Small, G. J.; Tiede, D. M. *J. Phys. Chem.* **1989**, *93*, 5953.